Expedited Articles

Novel Inhibitors of Carboxypeptidase G_2 (CPG_2): Potential Use in Antibody-Directed Enzyme Prodrug Therapy

Tariq H. Khan,*,† Ebun A. Eno-Amooquaye,† Frances Searle,† Pat J. Browne,§ Helen M. I. Osborn,‡ and Philip J. Burke§

Imperial College of Science, Technology and Medicine, Charing Cross Site, Medical Oncology, St. Dunstan's Road, London W6 8RF, U.K., Department of Chemistry, University of Reading, Whiteknights, Reading RG6 6AD, U.K., and Enzacta Ltd., Building 115, Porton Down Science Park, Salisbury, Wilts SP4 OJQ, U.K.

Received January 4, 1999

The design and synthesis of potent thiocarbamate inhibitors for carboxypeptidase G_2 are described. The best thiocarbamate inhibitor *N*-(*p*-methoxybenzenethiocarbonyl)amino-L-glutamic acid **6d**, chosen for preliminary investigations of in vitro antibody-directed enzyme prodrug therapy (ADEPT), abrogated the cytotoxicity of a combination of A5B7−carboxypeptidase G_2 conjugate and prodrug PGP (*N*-*p*-{*N*,*N*-bis (2-chloroethyl)amino}phenoxycarbonyl-L-glutamate) toward LS174T cells. This is the first report of a small-molecule enzyme inhibitor proposed for use in conjunction with the ADEPT approach.

Introduction

Nonspecific enzyme activity in the recently developed cancer treatment strategy, antibody-directed enzyme prodrug therapy (ADEPT), can be a serious limitation to such a potentially powerful method of cancer treatment. ADEPT has the advantage of being suitable for a wide range of cancers[1a−c] and was pioneered to enable selective delivery of cytotoxic agents to targeted tumors, via the use of antibody−enzyme conjugates.[2] In mice xenograft models,[3a] after optimum localization of the A5B7−carboxypeptidase G_2 (CPG_2) conjugate to the targeted tumors (typically 20 h), followed by slow plasma clearance of the excess conjugate (typically 52 h), a prodrug, which is a specific substrate for only the targeted enzyme, is administered. In theory, given sufficient time to allow the conjugate in the plasma and normal tissues to be removed, the subsequent generation of the cytotoxic drug occurs solely at the tumor site, eliminating nonlocalized toxicity.

In reality, after maximum tumor penetration by the antibody−enzyme conjugate, any attempt to administer the prodrug earlier than 72 h results in toxicity, particularly myelosuppression. Consequently, assisted strategies to remove excess circulating conjugate over the natural clearance mechanism are required. A successful approach would have the benefits of allowing early prodrug administration, at higher concentrations and for a much longer period of time. Assisted clearance has been achieved in animal models and clinically using an antibody (SB43) directed to the CPG_2 component of the antibody−enzyme conjugate. This antibody has also been galactosylated (SB43-gal), thus ensuring a more rapid and efficient plasma clearance of any antibody−enzyme conjugate to the liver by galactose receptors.[3b] This successful approach has allowed significant early reduction of enzyme activity in the serum, with minimal reduction of enzyme activity at the tumor site,[4] and consequently the prodrug may be administered 1 h after the galactosylated antibody (SB43-gal). A recent ADEPT clinical trial utilizing SB43-gal as a clearing agent confirms the importance of the assisted clearing step, by reducing the toxicity of the therapy. In addition, the greater sensitivity of the detection system used highlights the efficiency of this plasma clearing process with SB43-gal.[5]

In this paper we describe a possible cheaper, alternative, complementary refinement to ADEPT which may also allow early administration of prodrugs and result in minimal normal host tissue toxicity and maximum cancer therapy. This novel method of increasing the differential concentration of *activ*e enzyme between the tumor site and other normal host tissues involves the use of small-molecule enzyme-inactivating agents. Our strategy aims to chemically inhibit (preferably irreversibly) residual levels of non-tumor-localized enzyme while sustaining a sufficient quantity of the enzyme activity at the tumor site for therapy.

For this approach to be investigated inhibitors for CPG_2 had to be obtained. Consequently, we designed and synthesized a series of novel compounds which we hoped would inhibit the enzyme CPG_2, in both the free state and the conjugated state. The preparation and inhibitory properties of one successful series of compounds are presented in this paper.

Chemistry

A series of potential inhibitors for CPG_2 were initially designed, and these are shown in Table 1. A general chemical synthesis of the thiocarbamate derivatives is given in Scheme 1.

* To whom all correspondence should be sent.
† Imperial College of Science, Technology and Medicine.
‡ University of Reading.
§ Enzacta Ltd.

10.1021/jm990004i CCC: $18.00
Published on Web 03/04/1999

Scheme 1. General Synthesis of Thiocarbamate Derivatives **6** as Potential Inhibitors for CPG_2

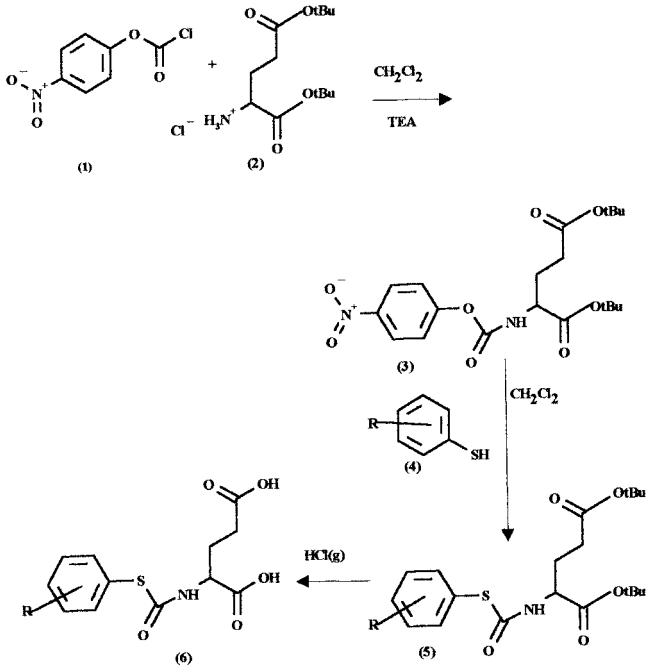

The synthetic strategy chosen involved *N*-activation with *p*-nitrophenyl chloroformate **1** of the α,γ-di-*tert*-butyl-L-glutamic acid hydrochloride derivative **2**, in the presence of triethylamine (TEA), to result in carbamate **3**. The crude activated glutamate derivative **3** was sufficiently pure to be used directly in the next stage, and subsequent treatment with a range of thiol compounds **4**, under argon or nitrogen, yielded, after column chromatography on silica gel, the purified coupled products **5**. The derivatives **5** were deprotected under acidic conditions to result in white precipitates **6**. These were usually sufficiently pure to be tested in the biological systems. Some of the derivatives were recrystallized from a mixture of hexane and ethyl acetate, and these proved hygroscopic and formed gums very easily after filtration or on standing. The final deprotected products **6** were characterized by ^{1}H NMR and thin-layer chromatography and were shown to be pure by combustion analysis. Table 1 shows the targets successfully synthesized together with their biological properties.

Biological Evaluation

The derivatives in Table 1 were tested in an in vitro cytotoxicity assay (IC_{50}) and also a Dixon plot (K_i) assay system. Generally these thiocarbamate derivatives were found to be nontoxic toward LS174T cells (>500 μM). Furthermore the apparent K_i ranged from 0.3 μM for **6d** to 165 μM for **6a**. Derivative **6d** was found to be the most potent CPG_2 inhibitor and had low toxicity to LS174T cells. Therefore, this was chosen as our optimum candidate for studying the detailed enzyme kinetics profile and an in vitro ADEPT investigation. The Lineweaver−Burk plots (Figure 2) and the apparent V_{max} and apparent K_m values listed in Table 2 show that V_{max} decreases with increasing concentration of **6d** and that the family of reciprocal plots intersects above the

Table 1. Structure and Biological Data for Potential Inhibitors of Carboxypeptidase G_2[c]

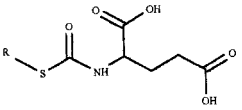

Code	Structure (R)	Formula	Ki (μM) [a]	IC_{50} (μM)[b]
6a		$C_{11}H_{12}N_2O_6S$	165	ND
6b		$C_{12}H_{14}N_2O_5S$	2.5	>500
6c		$C_{12}H_{14}N_2O_5S$	5.8	416
6d		$C_{13}H_{15}NO_6S$	0.30	>500
6e	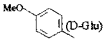	$C_{13}H_{15}NO_6S$	NC	>500
6f		$C_{13}H_{15}NO_6S$	1.07	>500
6g		$C_{13}H_{15}NO_5S$	1.05	>500
6h		$C_{13}H_{15}NO_5S.H_2O$	NC	>500
6i		$C_{12}H_{12}NO_5SBr$	NDI	ND
6j		$C_{12}H_{12}NO_5SCl$	NDI	ND

[a] Apparent inhibition. [b] Cytotoxicity toward LS174T cells. [c] NDI, no detectable inhibition; NC, not classical linear plot; ND, not determined.

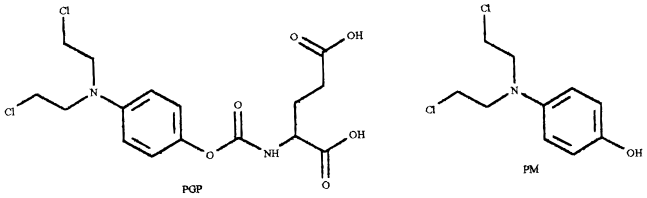

Figure 1. Structures of phenol mustard glutamate prodrug (PGP) and phenol mustard active drug (PM).

x-axis giving rise to different K_m values for each plot. These results suggest that **6d** exhibits noncompetitive inhibition with respect to methotrexate.

The ability of CPG_2 to activate a phenol mustard prodrug (PGP), Figure 1, was demonstrated by exposing LS174T cells to PGP in the presence of F(ab′)$_2$-A5B7−CPG_2. Figure 3 shows the dose−response curves for PGP against LS174T. The IC_{50} values obtained from the cytotoxicity assays are shown in Table 3. The LS174T cell line showed differential susceptibility to PGP alone (IC_{50} value of 23.22 ± 0.47 μM) and F(ab′)$_2$-A5B7−CPG_2 enzyme generated phenol mustard active drug (IC_{50} value of 0.8 ± 0.03 μM). The ability of **6d** to inhibit CPG_2 activity was evaluated by treating the cells with the conjugate F(ab′)$_2$-A5B7−CPG_2 and then simultaneously with PGP and a fixed concentration of **6d**. It was found that the cytotoxic activity derived from the prodrug in the presence of F(ab′)$_2$-A5B7−CPG_2 and **6d** was greatly diminished; however, in the absence of the conjugate F(ab′)$_2$-A5B7−CPG_2 co-administration of a mixture of

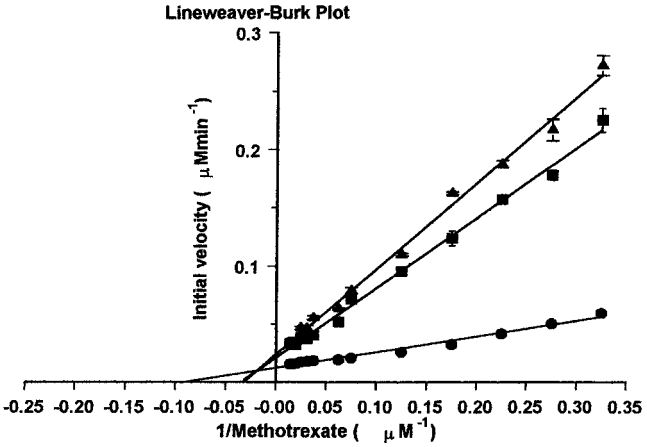

Figure 2. Lineweaver−Burk plot of the reciprocal of the initial reaction velocity (in units of min/μM) versus the reciprocal of methotrexate concentration at ●, methotrexate alone; ■, 0.5 μM **6d**; and ◆, 1.0 μM **6d**. CPG_2 concentration in the reaction solution was 0.2866 μg/mL.

Table 2. Apparent V_{max} and Apparent K_{max} Data from Lineweaver−Burk Plots of MTX Turnover by CPG_2 in the Presence of Inhibitor **6d**

concn of **6d** (μM)	V_{max}	K_m
0	79.99 ± 5.69	10 ± 0.76
0.5	47.66 ± 5.03	28.57 ± 0.64
1.0	42.28 ± 5.61	31.13 ± 0.89

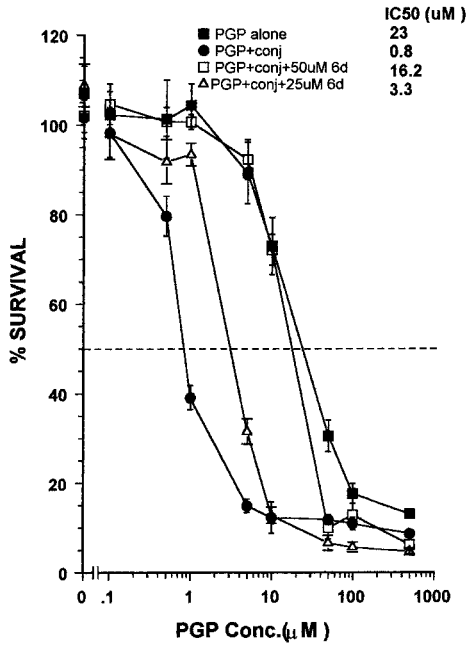

Figure 3. Dose−response curves of PGP on LS174T cells. The cells were treated as described in the Experimental Section. All cells were exposed to PGP for 1 h: ■, PGP alone; ●, $F(ab')_2$-A5B7−CPG_2 + PGP; △, $F(ab')_2$-A5B7−CPG_2 + PGP + **6d** (25 μM); □, $F(ab')_2$-A5B7−CPG_2 + PGP + **6d** (50 μM).

6d and PGP had little effect on the IC_{50} value of PGP alone (Table 3). In the presence of 25 μM **6d** the IC_{50} increased to 3.3 ± 0.19 μM and a 20-fold increase (IC_{50} 16.2 ± 0.66 μM) was observed in the presence of 50 μM **6d**. This shift toward higher IC_{50} values suggests that activation of prodrug is inefficient in the presence of **6d** and illustrates complete inhibition of CPG_2 activity by **6d**.

Table 3. Cytotoxicity Data for PGP Alone and Due to Conjugate Turnover of Prodrug PGP in the Presence of Inhibitor **6d** against LS174T Cells

	IC_{50} (μM)
PGP	23.22 ± 0.47
$F(ab')_2$-A5B7−CPG_2 + PGP	0.8 ± 0.03
$F(ab')_2$-A5B7−CPG_2 + PGP + **6d** (25 μM)	3.3 ± 0.19
$F(ab')_2$-A5B7−CPG_2 + PGP + **6d** (50 μM)	16.2 ± 0.66
PGP + **6d** (50 μM)	24.01 ± 0.46

Discussion

At the outset of this work no reports of any inhibitors for CPG_2 were known.[6] In addition no high-resolution X-ray crystallography data was available for this enzyme.[7] However, limited information was available concerning the closely related enzymes CPG and CPG_1. For example, it had already been demonstrated that certain peptides, notably *N*-(benzyloxycarbonyl)glutamate and *N*-benzoylglutamate, were moderate competitive inhibitors of CPG.[8] Our initial approach was to design inhibitors for CPG_2 which incorporated important structural features present in substrates for this enzyme, as displayed in recent publications.[9−11] A survey of the literature suggested that a free α-carboxylate moiety on the L-glutamate residue was essential for substrate specificity in the case of CPG_2; a benzene ring should lie in close proximity to the carbonyl group of the amide bond, as in folates and methotrexate,[12] but the linkage to the cleaved amide bond could vary between amide, carbamate, thiocarbamate, and urethane moieties.[13] It is well-established that two zinc ions are associated with each of the protein monomers of the dimeric enzyme, and these zinc ions are essential for the activity of this enzyme.[14] Since zinc ions have a high affinity for sulfur, protected sulfur moieties were incorporated within our compounds to potentially result in active-site-directed irreversible inhibitors.[15] Recent high-resolution crystallographic evidence, published during the course of this work,[16] confirmed that the zinc ions were indeed part of the active site of the enzyme.

Biodistribution studies on tissue concentrations of antibody−CPG_2 conjugate, prodrugs and active drugs of the benzoic acid mustard series in xenograft models,[17] have identified encouraging biodistribution properties which validate exploring small-molecule inhibitors for use in ADEPT. For example, the natural biodistribution of a benzoic acid mustard glutamate prodrug illustrates that, between 15 min and 4 h, higher concentrations of prodrugs occur in the liver, lung, and kidney than in the tumor xenografts.[3a] Furthermore, recent findings in tumor vascular architecture research have illustrated that due to local flow-limited transport, plasma-borne agents are poorly delivered to tumors.[18] *Therefore, these results argue that, provided the biological distribution of the inhibitor is similar to that of the prodrug, greater concentrations of the inhibitor will be available for inhibition of the residual enzyme in normal tissues than are required to fully suppress all the enzyme activity at the tumor.* This should allow administration of a high concentration of prodrugs without causing any myelosuppression, immediately after inhibition of the conjugate in the plasma, thus allowing a completely intact immune system to function together with the ADEPT strategy to eradicate the tumor.

Our first series of potential inhibitors incorporated a thiocarbamate functionality (Scheme 1). This work with the thiocarbamate derivatives, Table 1, has shown that the ability to inhibit CPG_2 is sensitive to substituent variations on the benzene ring and also the chirality of glutamic acid. On comparing the lipophilic *para*-substitution (**6d**,**g**) with the lipophilic *meta*-substitution (**6f**,**h**), we find that the *para*-substituted derivatives are consistently better inhibitors than the *meta*-substituted derivatives. By placing hydrophilic functional groups in the *para*-position of the benzene ring of the thiocarbamate derivative, inhibition efficiency is reduced by a factor of at least 6 compared to the lipophilic moieties (**6d**). Furthermore, inhibitory properties cannot be improved by replacing the phenyl ring by a pyridyl ring, as in **6a**. On forming the *N*-oxide **6a** of the pyridyl compound, the inhibitory properties are again further reduced by a factor of 60 compared to **6d**. The presence of electron-withdrawing groups (Br **6i**, Cl **6j**) on the benzene ring destabilizes the thiocarbamate bond to such an extent that no enzyme inhibition is observed. It is concluded that the rate of hydrolysis is too rapid in the aqueous media for these particular derivatives to exert an inhibitory effect on CPG_2. The rate of hydrolysis of the thiocarbamate linkage may partly explain the low inhibitory properties of the pyridyl *N*-oxide derivative. The electron-deficient pyridyl ring activates the thiocarbamate bond to hydrolysis in aqueous media. This would suggest electron-donating substituents on the phenyl ring would stabilize the thiocarbamate bond, thereby making the derivative a good inhibitor. Electron-donating moieties on the phenyl ring, such as **6d**−**h**, were found to have much better inhibitor properties. In addition, the chirality of glutamic acid, for example, in **6e,** the D-isomer of **6d**, is very important for obtaining the correct interaction with the enzyme active site. The *p*-methoxy derivative **6d** was found to have the best overall properties from all the thiocarbamate derivatives synthesized.

Incubation of 50 μM **6d** in a cell culture assay in the presence of CPG_2 (0.2866 μg/mL) has shown that the inhibitor can remove practically all toxic effects due to the turnover of the potent phenol mustard prodrug (PGP).

Conclusions

In this work a novel noncompetitive inhibitor **6d** of CPG_2 has been discovered. This suggests that **6d** is an ideal candidate to test the novel hypothesis of using small-molecule inhibitors as an enzyme-clearing strategy in antibody-directed enzyme prodrug therapy in vivo.

Experimental Section

NMR spectra were determined on a 250-MHz Brucker instrument (ULIRS, Queen Mary and Westfield College) with chemical shifts (δ) reported relative to Me_4Si. TLC was performed on Merck aluminum sheets silica gel F_{254} (Art. 5554); spots were visualized under 254- and 365-nm UV light and with the aid of ninhydrin (0.1% w/v in acetone) or bromophenol blue (0.1% w/v in ethanol) solutions. In some cases the use of sodium periodate (1% w/v in distilled water) and heat was used to identify easily oxidizable species. Column chromatography was carried out on Merck 1.09385 silica gel 60 (230−400 mesh). Melting points were measured on a Gallenkamp capilliary melting point apparatus and are not corrected. Microanalyses were performed by C.H.N. Analysis Ltd., Alpha House, Countesthorpe Road, South Wigston, Leicester LE8 2PJ, U.K. Chemicals were purchased from Aldrich, The Old Brickyard-New Road-Gillingham-Dorset SP8 4XT, England. Di-*tert*-butyl-L-glutamic acid hydrochloride was obtained from BaChem or Sigma, Poole.

Solvents were used as commercially available. However, where dry solvents were required a drying agent, such as calcium hydride, was used to dry the solvent by refluxing the solvent in the presence of the drying agent for 1−2 h in an inert atmosphere, followed by distillation at atmospheric pressure.

General Synthetic Procedure for Thiocarbamate Derivatives, Scheme 1. Di-*tert*-butyl-L-glutamic acid HCl salt **2** (2.05 g, 6.95 mmol) was activated by addition of *p*-nitrophenyl chloroformate **1** (1.4 g, 6.95 mmol) in dry dichloromethane (20 mL) in the presence of triethylamine (2 mL, 14.4 mmol). The reaction mixture was heated under reflux for 25 min and then stirred for 1 h at room temperature. The reaction mixture, containing mainly the *N*-activated glutamic acid derivative **3,** was flushed with argon, and then a solution of the thiol **4** (7.70 mmol) in dichloromethane (20 mL) was added and heated to reflux for 10 min. The cooled solution was then stirred for 5 h at room temperature and monitored by TLC for disappearance of starting material. The reaction mixture was concentrated in vacuo and then stirred with ethyl acetate for 30 min; the precipitate was filtered and the filtrate concentrated in vacuo. The crude residue was chromatographed on silica gel (CH_2Cl_2). The fully protected derivative **5** was isolated as a colorless oil, which was dissolved in hexane or CH_2Cl_2 (30 mL), treated with HCl(g), and stirred at room temperature overnight. The diacid product **6**, a white precipitate, was filtered, washed with hexane or CH_2Cl_2, and dried in vacuo to result in the analytically pure thiocarbamate derivatives **6** (Scheme 1).

***N*-(*p*-Thiopyridinylcarbonyl-*N*-oxide)-L-Glutamic Acid (6a).** *p*-Thiopyridine was dissolved in dichloromethane (10 mL) and added to the *p*-nitrophenyl-activated di-*tert*-butylglutamic acid intermediate **3**. The reaction mixture was stirred at room temperature and monitored by TLC; after all the starting material had reacted the reaction mixture was treated with 1 equiv of *m*-chloroperbenzoic acid and stirred for 24 h. The reaction mixture was concentrated in vacuo and chromatographed on silica. The purified protected product **5a** was treated with gaseous hydrogen chloride and stirred for 48 h. The solution was concentrated in vacuo to result in a white precipitate. Trituration with ethyl acetate (to remove *m*-chlorobenzoic acid) resulted in a hygroscopic white solid **6a**. Anal. ($C_{11}H_{12}N_2O_6S$) C,H,N.

***N*-(*m*-Aminophenylthiocarbonyl)-L-glutamic Acid (6b).** Modification to the general procedure: The final acidification deprotection step involved a mixture of 1:5 methanol:dichloromethane and gaseous dry hydrogen chloride. A yellow solid precipitated out of the reaction mixture; this was filtered and dried. The impurity was removed by crystallization from hot methanol and ethyl acetate. The required product **6b** was isolated from the filtrate on concentration in vacuo, as an orange gum. The product was found to be hygroscopic. Anal. ($C_{12}H_{14}N_2O_5S$·0.2EtOAc) C,H,N.

***N*-(*p*-Aminophenylthiocarbonyl)-L-glutamic Acid (6c).** Modification to the general procedure: The final acidification deprotection step involved a mixture of 1:5 methanol:dichloromethane and gaseous hydrogen chloride. A yellow solid precipitated out of the reaction mixture; this was filtered and dried. The impurity was removed by crystallization from hot methanol and ethyl acetate. The required product **6c** was isolated from the filtrate on concentration in vacuo, as an orange gum. The product **6c** was found to be hygroscopic. Anal. ($C_{12}H_{14}N_2O_5S$·0.2EtOAc) C,H,N.

***N*-(*p*-Methoxyphenylthiocarbonyl)-L-glutamic acid (6d):** ^{1}H NMR (250 MHz, DMSO-d_6) δ 8.20 (1H, d, J = 8.0 Hz, NH), 7.10 (2H, d, J = 8.0 Hz, ArH), 6.7 (2H, d, J = 8.0 Hz, ArH), 3.9 (1H, m, CH), 3.5 (3H, s, OMe), 2.1 (2H, m, CH_2), 1.6 (2H, m, CH_2); mp 115 °C; HPLC stability studies indicated a $t_{1/2}$ of

34 min in phosphate buffer at pH 7.3 and 37 °C.[19] Anal. ($C_{13}H_{15}NO_6S$) C,H,N.

***N*-(*p*-Methoxyphenylthiocarbonyl)-D-glutamic acid (6e):** ^{1}H NMR (250 MHz, DMSO-d_6) δ 8.20 (1H, d, J = 8.0 Hz, NH), 7.10 (2H, d, J = 8.0 Hz, ArH), 6.7 (2H, d, J = 8.0 Hz, ArH), 3.9 (1H, m, CH), 3.5 (3H, s, OMe), 2.1 (2H, m, CH_2), 1.6 (2H, m, CH_2); mp 110 °C. Anal. ($C_{13}H_{15}NO_6S$) C,H,N.

***N*-(*m*-Methoxyphenylthiocarbonyl)-L-glutamic acid (6f):** ^{1}H NMR (250 MHz, DMSO-d_6) δ 8.80−6.60 (5H, m, ArH, NH), 4.10 (1H, m, CH), 3.65 (3H, s, OMe), 2.40−1.60 (4H, m, $[CH_2]_2$). Anal. ($C_{13}H_{15}NO_6S$) C,H,N.

***N*-(*p*-Methylphenylthiocarbonyl)-L-glutamic acid (6g):** ^{1}H NMR (250 MHz, DMSO-d_6) δ 12.4−12.5 (2H, b, COOH), 8.55(1H, d, CONH), 7.35 (2H, d, J = 8 Hz, ArH), 7.24 (2H, d, J = 8 Hz, ArH), 4.27−4.14 (1H, m, CH), 2.40−2.22 (5H, m, $CH_3 + CH_2$), 2.09−1.92 (1H, m, CH_2), 1.91−1.73 (1H, m, CH_2). Anal. ($C_{13}H_{15}NO_5S$) C,H,N.

***N*-(*m*-Methylphenylthiocarbonyl)-L-glutamic acid (6h):** ^{1}H NMR (250 MHz, DMSO-d_6) δ 12.4−12.5 (2H, b, COOH), 8.60 (1H, d, CONH), 7.34−7.19 (4H, m, ArH), 4.26−4.14 (1H, m, CH), 2.38−2.24 (5H, m, CH_3 +CH_2), 2.09−1.92 (1H, m, CH_2), 1.90−1.73 (1H, m, CH_2). Anal. ($C_{13}H_{15}NO_5S\cdot H_2O$) C,H,N.

***N*-(*p*-Bromophenylthiocarbonyl)-L-glutamic acid (6i):** ^{1}H NMR (250 MHz, DMSO-d_6) δ 12.4−12.5 (2H, b, COOH), 8.71 (1H, d, CONH), 7.61 (2H, d, J = 8 Hz, ArH), 7.42 (2H, d, J = 8 Hz, ArH), 4.27−4.14 (1H, m, CH), 2.39−2.29 (2H, m, CH_3 +CH_2), 2.09−1.91 (1H, m, CH_2), 1.91−1.73 (1H, m, CH_2). Anal. ($C_{13}H_{12}NO_5SBr$) C,H,N.

***N*-(*p*-Chlorophenylthiocarbonyl)-L-glutamic acid (6j):** ^{1}H NMR (250 MHz, DMSO-d_6) δ 12.4−12.5 (2H, b, COOH), 8.71 (1H, d, CONH), 7.49 (4H, s, ArH), 4.28−4.16 (1H, m, CH), 2.38−2.28 (2H, m, $CH_3 + CH_2$), 2.09−1.91 (1H, m, CH_2), 1.91−1.73 (1H, m, CH_2). Anal. ($C_{13}H_{12}NO_5SCl$) C,H,N.

All of the synthesized compounds (Table 1) were then tested to determine their CPG_2 inhibitory properties using the Dixon plot. The Dixon plot was chosen for the preliminary screen to determine the apparent K_i.[20] In addition, the cytotoxicity (IC_{50}) of each compound was also determined.

Determination of Apparent K_i. Assay solutions were set up with varying inhibitor concentrations (0−3.0 μM) at different concentrations of methotrexate; 10 μL (0.1 U) of stock enzyme solution was dispensed into 1-mL cuvettes, and reaction was started by the addition of 990 μL of assay solutions.

Enzyme solution (10 μL) was dispensed into 1-mL cuvettes, and inhibitor solutions (990 μL) were added. The initial rate of decrease of absorbance was measured spectrophotometrically at 320 nm in a Shimadzu UV 1601 spectrophotometer. The reciprocal of the initial velocity, 1/V, was plotted against the micromolar (μM) concentrations of inhibitor to give the linear Dixon plot [20] from which apparent K_i was obtained, as shown in Table 1.

Biological Studies. 1. Cell Line. The human colon adenocarcinoma cell line, LS174T, which expresses carcinoembryonic antigen (CEA) was obtained from the European Animal Cell Culture Collection.

2. Enzyme and Antibody−Enzyme Conjugate. Bacterial enzyme CPG_2 and a conjugate of the F(ab′)$_2$ fragment of the mouse anti-CEA antibody, A5B7, and the antibody enzyme conjugate (F(ab′)$_2$-A5B7−CPG_2) were kindly provided by Dr. R. G. Melton, Division of Biotechnology, Centre for Applied Microbiology and Research, Porton Down, Salisbury, Wilts, SP4 OJG, U.K.

The most promising of the compounds listed in Table 1 were then subjected to screening against LS174T cell lines for their capacity to abrogate in vitro cytotoxicity in the presence of enzyme and the prodrug *N*-*p*-[bis(2-chloroethyl)amino]phenoxycarbonyl-L-glutamic acid (PGP), Figure 1.

Compound **6d** was chosen due to its low toxicity and best inhibition of CPG_2 and was thus studied in depth, to determine its mode of inhibition and its capacity to suppress enzyme activity in vitro.

3. Kinetics. All kinetics were performed at 37 °C in 0.1 M Tris-HCl, pH 7.3, buffer containing 0.1 mM zinc chloride (assay buffer). CPG_2 (38.13 mg/mL, 350 U/mg) was diluted in assay buffer to make a stock solution of 28.66 μg/mL; 10 U/mL concentrations shown in the text are final concentrations after all the incubation solutions are combined. One unit of CPG_2 activity corresponds to 1 μmol of methotrexate hydrolyzed min^{-1}.[21] All values for the initial velocity were calculated from the progress curve using the computer-assisted spectrophotometer (molar extinction coefficient of methotrexate is 8300). Hyperbolic saturation curves were obtained by measuring CPG_2 activity at varying methotrexate concentration and different fixed **6d** concentration. Methotrexate concentration was varied between 3.077 and 70 μM, while **6d** was at fixed concentrations of 0.5 and 1.0 μM; 10 μL of stock CPG_2 was placed in a 1-mL cuvette, the reaction was initiated by adding 990 μL of methotrexate alone or methotrexate containing **6d**, and the decrease in absorbance at 320 nm was recorded over a time interval of 0−60 s. To obtain values for apparent K_m and apparent V_{max}, the data was fitted by the least-squares fit to the Michaelis−Menten equation using Fig.P (Biosoft) computer program. The pattern of **6d** inhibition with respect to methotrexate was illustrated by using a double-reciprocal (Lineweaver−Burk) plot of the data. Concentrations shown in the text are final concentrations after all the incubation solutions are combined.

Cytotoxicity Studies. 1. General Method for Cytotoxicity of Potential CPG_2 Inhibitors. To determine cytotoxicity of the inhibitor, cells were incubated with graded concentration of inhibitor for 1 h at 37 °C. The cytotoxicity of each potential inhibitor against LS174T cells was also determined by exposing the cells to graded concentrations of particular inhibitor (0.01−500 μM in medium) for 1 h at 37 °C. After each treatment the cells were washed once with medium and incubated for a further 6 days. Cell survival for all the experiments was measured by the SRB assay.[22]

2. In Vitro Inhibition of CPG_2 Activation of Prodrug (PGP) by 6d. To demonstrate in vitro inhibition of CPG_2 turnover of prodrug (PGP), Figure 1, in the presence of **6d**, LS174T cells were treated as follows: (a) To determine the cytoxicity of parent drug (phenol mustard) produced in situ by the action of the antibody−enzyme conjugate, the cells were incubated with 100 μL of F(ab′)$_2$-A5B7−CPG_2 (3.32 μg/mL, 0.505 U/mL) at 37 °C for 1 h. The cells were then washed two times in 200 μL of medium to remove excess conjugate which had not bound to the cells, followed by incubation with 200 μL of graded concentration of prodrug (PGP) (0.01−500 μM in medium) for 1 h at 37 °C. (b) To determine inhibition of cytotoxicity in the presence of **6d**, the cells were incubated with 100 μL of F(ab′)$_2$-A5B7−CPG_2 (3.32 μg/mL, 0.505 U/mL) for 1 h at 37 °C. The cells were then washed two times in 200 μL of medium to remove unbound conjugate, followed by incubation with graded concentration of PGP plus 25 or 50 μM **6d** for 1 h at 37 °C. (c) To determine cytotoxicity of the PGP alone, this was carried out as described above for the potential inhibitors.

Acknowledgment. We are very grateful to Dr. G. Rogers, Dr. R. G. Melton, Dr. R. Sherwood, and Prof. R. J. Knox for their kind assistance. We also thank Enzacta Ltd. for financial support.

References

(1) (a) Melton, R. G.; Sherwood, R. F. Antibody-Enzyme conjugates for therapy (Review). *J. Natl. Cancer Inst.* **1996**, *88*, 153−165. (b) Melton, R. G.; Connors, T.; Knox, R. J. The use of Prodrugs in Targeted Anticancer Therapies. *STP Pharma Sci.* **1999**, in press. (c) *Enzyme-prodrug strategies for cancer therapy*; Melton, R. G., Knox, R. J., Eds.; Plenum: London, 1999; in press.

(2) Bagshawe, K. D. Antibody directed enzymes revive anti-cancer prodrugs concept. *Br. J. Cancer* **1987**, *56*, 531−532.

(3) (a) Antoniw, P. A study of the pharmacology of different prodrugs in conjunction with targeted antibody-enzyme conjugate in human cancer therapy. Ph.D. Thesis, University of London, Charing Cross and Westminter Medical School, London, U.K., 1991. (b) Sharma, S. K.; Bagshawe, K. D.; Burke, P. J.; Boden, J. A.; Rogers, G. T.; Springer, C. J.; Melton, R. G.; Sherwood, R. F. Galactosylated antibodies and antibody-enzyme conjugates in antibody-directed enzyme prodrug therapy. *Cancer* **1994**, *73*, 1114−1120.

(4) Rogers, G. T.; Burke, P. J.; Sharma, S. K.; Koodie, R.; Boden, J. A. Plasma clearance of an antibody-enzyme conjugate in ADEPT by monoclonal anti-enzyme: its effect on prodrug activation in-vivo. *Br. J. Cancer* **1995,** *72(6),* 1357−1363.
(5) Martin, J.; Stribbling, S. M.; Poon, G. K.; Begent, R. H. J.; Napier, M.; Sharma, S. K.; Springer, C. J. Antibody-directed enzyme prodrug therapy: pharmacokinetics and plasma levels of prodrug and drug in a phase I clinical trial. *Can. Chem. Pharmacol.* **1997**, *40*, 189−201.
(6) Hughes, P.; Sherwood, R. F.; Lowe, C. R. A single report for the use of triazine dye, Procion red MX-8B, for the use of affinity labeling of CPG_2 at the active site has been published. Studies on the nature of transition-metal-ion-mediated binding of triazine dyes to enzymes. The interaction of procion red MX-8B with carboxypeptidase G_2. *Eur. J. Biochem.* **1984**, *144*, 135−142.
(7) Lloyd, L. F.; Collyer, C. A.; Sherwood, R. F. Crystallization and preliminary crystallographic analysis of carboxypeptidase G_2 from *Pseudomonas sp*. strain RS-16. *J. Mol. Biol.* **1991**, *220*, 17−18.
(8) Goldman, P.; Levy, C. C. Carboxypeptidase G: purification and properties. *Proc. Nat. Acad. Sci. U.S.A.* **1967**, *58*, 1299.
(9) Blakey, D. C.; Valaccia, B. E.; East, S.; Wright, A. F.; Boyle, F. T.; Springer, C. J.; Burke, P. J.; Melton, R. G.; Bagshawe, K. D. Antitumor effects of an antibody-carboxypeptidase G_2 conjugate in combination with benzoic acid mustard prodrug. *Cell Biophys.* **1993**, *22(1−3)*, 1−8.
(10) Blakey, D. C.; Davies, D. H.; Dowell, R. I.; East, S. I.; Burke, P. J.; Sharma, S. K.; Springer, C. J.; Mauger, A. B.; Melton, R. G. Anti-tumour effects of an antibody-carboxypeptidase G2 conjugate in combination with phenol mustard prodrugs. *Br. J. Cancer* **1995**, *72(5)*, 1083−1088.
(11) Springer, C. J.; Dowel, R.; Burke, P. J.; Hadley, E.; Davis, D. H.; Blakey, D. C.; Melton, R. G.; Niculescu-Duvaz, I. Optimisation of alkylating agent prodrugs derived from phenol and aniline mustards: a new clinical candidate prodrug (ZD2767) for antibody-directed enzyme prodrug therapy (ADEPT). *J. Med. Chem.* **1995**, *38*, 5051−5065.
(12) DeAngelis, L. M.; Tong, W. P.; Lin, S.; Fleisher, M.; Bertino, J. R. Carboxypeptidase G_2 rescue after high-dose methotrexate. *J. Clin. Oncol.* **1996**, *14 (7)*, 2145−2149.
(13) Dowell, R. I.; Springer, C. J.; Davies, D. H.; Hadley, E. M.; Burke, P. J.; Boyle, T. F.; Melton, R. G.; Connors, T. A.; Blakey, D. C.; Mauger, A. B. New Mustard prodrugs for antibody-directed enzyme prodrug therapy: Alternatives to the amide link. *J. Med. Chem*, **1996**, *39*, 1100−1105.
(14) McCullough, J. L.; Chabner, B. A.; Bertino, J. R. Purification and properties of carboxypeptidase G_1. *J. Biol. Chem.* **1971**, *246 (23)*, 7207−7213.
(15) Ruf, M.; Weis, K.; Brasack, I.; Vahrenkamp, H. Modelling transition state analogues and enzyme−inhibitor complexes of zinc-containing class II aldolases and metalloproteases. *Inorg. Chim. Acta* **1996**, *259*, 271−281.
(16) Roesell, S.; Pauptit, R. A.; Tucker, A. D.; Melton, R. G.; Blow, D. M.; Brick, P. Crystal structure of carboxypeptidase G_2, a bacterial enzyme with application in cancer therapy. *Structure* **1997**, *5(3)*, 337−347.
(17) Antoniw, P.; Springer, C. J.; Bagshawe, K. D.; Searle, F.; Melton, R. G.; Rogers, G. T.; Burke, P. J.; Sherwood, R. F. Disposition of the prodrug 4-(bis(2-chloroethyl)amino)benzoyl-L-glutamic acid and its active parent drug in mice. *Br. J. Cancer* **1990**, *62*, 909−914.
(18) Baish, J. W.; Gazit, Y.; Berk, D. A.; Nozue, M.; Baxter, L. T.; Jain, R. K.Role of tumor vascular architecture in nutrient and drug delivery: an invasion percolation-based network model. *Microvasc. Res.* **1996**, *51(3)*, 327−346.
(19) A time course HPLC analysis was carried out by Prof. R. J. Knox on a Waters HPLC system using C_{18} reversed-phase silica gel analytical column, UV detector, and methanol as eluent, to evaluate $t_{1/2}$ for the most useful inhibitor.
(20) Dixon, M. The determination of K_m and K_i. *Biochem. J.* **1972**, *129(1)*, 197−202.
(21) Sherwood, R. F.; Melton, R. G.; Alwan, S. M.; Hughes, P. Purification and properties of carboxypeptidase G2 from *Pseudomonas sp*`. Strain RS-16. Use of a novel triazine dye affinity method. *Eur. J. Biochem.* **1985**, *148(3)*, 447−453.
(22) Skehan, P.; Storeng, R.; Scudiero, D.; Monks, A.; McMahon, J.; Vistica, D.; Warren, J. T.; Bokesch, H.; Kenney, S.; Boyed, M. R. New colorimetric cytotoxicity assay for anti-cancer drug screening. *J. Natl. Cancer Inst.* **1990**, *82*, 1107−1112.

JM990004I